Supplemental Figure Legends:

Figure S1: Characterization of reduced mTOR expression in the mTOR$^{\Delta/\Delta}$ mice. A) Western blot analysis of mTOR expression in the heart and pancreas of two wild type and two mTOR$^{\Delta/\Delta}$ mice. Actin or GAPDH are used as loading controls. B) Immunoprecipitation of mTOR from MEF protein lysate. Co-immunoprecipitation of Raptor or Rictor is evidence of the level of TORC1 and TORC2 complex formation. Input Western blot demonstrates reduction in overall mTOR expression without discernable effect on Raptor or Rictor expression. Tubulin is used as a loading control for the input lysates. C) Assessment of global protein synthesis. Rates of ^{35}S-methionine incorporation were determined over the indicated time frame in MEFs initially obtained from WT (mTOR$^{+/+}$) or mTOR$^{\Delta/\Delta}$ embryos. D) Tumor incidence observed at the time of necropsy for WT and mTOR$^{\Delta/\Delta}$ mice (WT, n=26 and mTOR$^{\Delta/\Delta}$ mice, n=36). E) Tumor incidence as a function of genotype and sex. For WT mice, we observed that 10/26 mice developed tumors (6F/4M). For mTOR$^{\Delta/\Delta}$ mice, we noted 8/36 developed tumors (6F/2M).

Figure S2: Metabolic effects of reduced mTOR expression. A) Body composition of mTOR$^{\Delta/\Delta}$ mice is not altered when compared to wild type mice. Various tissues were obtained at sacrifice, individually weighed and expressed as a percentage of overall body weight. Tissues assayed include liver, heart, pancreas, epididymal white adipose tissues (EWAT) and brown adipose tissue (BAT). (n=9 male mice per genotype, no significant differences were observed). B) Levels of fasting serum insulin in young WT (n= 7, shaded bars) or mTOR$^{\Delta/\Delta}$ mice (n=6, open bars). C) Glucose stimulated insulin secretion (GSIS) of islets isolated from young WT (shaded bars) or mTOR$^{\Delta/\Delta}$ mice (open bars). Islets were stimulated with either 3 mM or D) 16.7 mM extracellular glucose and insulin levels determined in the supernatant and subsequently normalized to islet DNA concentration. Shown is the average of two independent experiments each performed in triplicate with *p<0.05. E) Glucose tolerance test in old male wild type and mTOR$^{\Delta/\Delta}$ mice (n=4 per genotype). F) Young mice (age 2-3 months) were analyzed for F) free fatty acid (FFA) levels. Shown are the values for WT mice (shaded bars, n=7) and mTOR$^{\Delta/\Delta}$ mice (open bars, n=6). G) Serum triglycerides levels (n=7 WT and n=6 mTOR$^{\Delta/\Delta}$) and H) serum adiponectin levels (n=6 WT and n=6 mTOR$^{\Delta/\Delta}$). All metabolic experiments were performed in male mice.

Figure S3: Biomarkers of aging are reduced in mTOR$^{\Delta/\Delta}$ mice. A) Representative nitrotyrosine staining in old WT or mTOR$^{\Delta/\Delta}$ myocardial tissue. Top row is assessed for nitrotyrosine levels (red) while the bottom row represents a DAPI nuclear counterstain (blue). B) Quantification of nitrotyrosine staining in old WT or mTOR$^{\Delta/\Delta}$ heart tissues. Analysis involved four mice per genotype using the average of 3-5 random sections per mouse. C) Polyubiquitin staining in sections obtained from old WT or mTOR$^{\Delta/\Delta}$ myocardium. Top row is a representative assessment for polyubiquitin levels (red) while the bottom row is the DAPI nuclear counterstain (blue). D) Quantification of polyubiquitin accumulation in old WT or mTOR$^{\Delta/\Delta}$ heart tissues. Analysis involved four mice per genotype using the average of 3-5 random sections per mice. *p<0.05

Figure S4: Physiological characterization of reduced mTOR expression. A) Rotarod speed analysis for wild type and $mTOR^{\Delta/\Delta}$ male mice. Analysis of maximum Rotarod speed obtained as a function of age and genotype is shown. No differences were observed between young wild type (shaded bars, n=6 male mice) or $mTOR^{\Delta/\Delta}$ mice (open bars, n=6 male mice). Maximum speed obtainable was reduced in old WT mice (n=4 male mice) and old $mTOR^{\Delta/\Delta}$ mice (n=7 male mice), although the $mTOR^{\Delta/\Delta}$ mice had significantly better performance; *$p<0.05$. B) Representative histology of the testes of WT or C) $mTOR^{\Delta/\Delta}$ mice that were both 31 months of age. No clear differences were observed in these animals or in four other mice analyzed. D) Rates of cataract formation as analyzed by histological sections obtained from mice sacrificed at 21 months (3 WT and 3 $mTOR^{\Delta/\Delta}$ female mice) or at 31 months (3 WT and 3 $mTOR^{\Delta/\Delta}$ male mice).

Extended Experimental Procedures

Body Composition

The weight of male $mTOR^{+/+}$ and $mTOR^{\Delta/\Delta}$ mice were monitored weekly for 20 weeks beginning 7 days after birth. Food intake was analyzed over a one week period using individually housed 10 week old male $mTOR^{+/+}$ and $mTOR^{\Delta/\Delta}$ mice. Body composition was performed by sacrificing mice and determining the excised wet weight of individual tissues and organs normalized to overall body weight.

Western Blot, Gene expression and Histochemical analysis:

Mouse embryonic fibroblasts (MEFs) were prepared from E12-E14 day old embryos using standard methods. MEFs were prepared from embryos resulting from $mTOR^{\Delta/+}$ breeders. MEFs were cultured in growth medium consisting of Dulbecco's Modified Eagle's medium (DMEM; Invitrogen) supplemented with 15% fetal bovine serum (FBS), 50 units/ml penicillin and 50 μg/ml streptomycin. Where indicated, primary MEFs at passage 2-4 were cultured in RPMI Leucine-free media (MP Biomedical) supplemented with 15% dialyzed FBS (Invitrogen) for 2 hours prior to stimulation with 52 μg/ml L-leucine (Sigma).

Primary MEFs were lysed with Nonidet P-40 Lysis buffer (1.0% Nonidet P-40, 50 mM Tris-HCl pH 7.4, 150 mM NaCl, 5 mM EDTA) supplemented with protease inhibitor tablet (Roche) and phosphatase inhibitors (1 mM Na_3VO_3, 1 mM β-glycerolphosphate, 10 mM NaF) for 15 min on ice prior to clarification by centrifugation at 16,100 x *g* for 15 min at 4 °C. Tissues were either homogenized in Nonidet P-40 Lysis buffer or in homogenizing buffer (25 mM Tris HCl pH 7.4, 150 mM NaCl, 5 mM EDTA, 1% Triton X-100, 0.1% SDS, 10% glycerol, 1 mM DTT, 0.5 % sodium deoxycholic acid) supplemented with protease and phosphatase inhibitors using a Tissue Lyser homogenizer (Qiagen). Protein concentration was determined with the Pierce BCA assay Kit (Thermo Fisher Scientific). Protein lysates were resolved on precast Tris-Glycine SDS gels (Invitrogen) and transferred onto nitrocellulose membranes. Immunoblot analysis was performed with the following antibodies: phospho-AKT (Cell Signaling), phospho-S6K (Cell Signaling), mTOR (Cell Signaling), Akt (Santa Cruz Biotechnology), S6K (Santa Cruz Biotechnology), Raptor (Cell Signaling), Rictor (Cell Signaling), actin (Sigma), and GAPDH (Santa Cruz Biotechnology). For analysis of mTOR complex formation, MEF cells were lysed in Complex Lysis buffer (40 mM HEPES [pH 7.4], 2mM EDTA, 10 mM pyrophosphate, 10 mM glycerophosphate, and 0.3% CHAPS, supplemented with protease inhibitor tablet (Roche)) and placed on ice for 30 min followed by centrifugation at 13,000 rpm for 10 min at 4 °C. For immunoprecipitation, cell lysates (200 μg total protein) were incubated with an anti-mTOR antibody (2 μg, Santa Cruz Biotechnology, sc-1549) for 3 hours at 4°C. Protein G-sepharose (Amersham) was added, and the lysate was subsequently incubated overnight at 4°C on a rotating platform. Immunocomplexes were collected by centrifugation, washed three times with Complex Lysis buffer containing 150 mM NaCl, and resolved on precast 3-

8% Tris-Acetate gels (Invitrogen). Gels were transferred onto nitrocellulose membranes and probed with Raptor, Rictor or mTOR antibodies as denoted above.

For assessment of protein translation rates, MEF cells **were** grown in 12-well plates and incubated for the indicated time with 50 µCi /ml of [^{35}S]-methionine (PerkinElmer) in methionine free RPMI medium. Cells were then lysed and all proteins were precipitated by incubation with 10% trichloroacetic acid (TCA) for 30 minutes on ice. The precipitated proteins were collected by centrifugation, washed twice with 100% acetone, air dried and then resuspended with RIPA buffer. The methionine incorporation was determined by a liquid scintillation counter and the protein synthesis rates expressed as count per minute (cpm) per thousand cells.

For the *in vivo* assessment of mTOR activity, 20-24 week old male mice that had been fasted overnight were intraperitoneally injected with insulin or saline (control) as previously described (Wu et al., 2006). Briefly, ten minutes after injection, mice were euthanized, tissues were snap frozen in liquid nitrogen and samples processed in Nonidet P-40 Lysis buffer as described above. Levels of p16^{Ink4A} mRNA were determined from mouse tissues by quantitative RT-PCR using the strategy and primers that were described previously (Liu et al., 2009).

Histological analysis was performed on tissues isolated from young WT mice (2-3 months old) or old WT (n=3, one female and 2 males, mean age 24.5 ± 1.6 months) or old mTOR$^{\Delta/\Delta}$ mice (n=4, 2 female and 2 male, mean age 24.7 ± 2.0 months). Cryostat sections were prepared and fixed with 4% paraformaldehyde in PBS prior to immunohistochemical analysis with either a nitrotyrosine antibody (Millipore) or polyubiquitin antibody (Enzo Life Sciences) using standard protocols. For brain sections, the tissue was cut in 10 µm thick coronal sections. Fluorescent images were obtained using a Zeiss Axioskop 2 Plus and fluorescence intensities were measured by image J analysis. Three to five random sections were analyzed per tissue per mouse.

Metabolic Testing:

Glucose and Insulin Tolerance testing was performed according to standard procedures. Blood glucose was determined using a one-touch Ascensia Elite glucometer (Fisher). Insulin levels were measured by radioimmunoassay according to the manufacturer's recommendation (Millipore). For glucose stimulated insulin secretion (GSIS), the bile ducts of 8-12 week old male mice were perfused with a 0.5 mg/ml collagenase V/Hank's Buffered Salt Solution (HBSS; Sigma). Collagenase-perfused organs were isolated and incubated at 37ºC for 20-30 minutes. HBSS supplemented with 1% FBS was added to stop the digestion. Digested tissues were vortexed and filtered through 1.5mm metal mesh. Histopaque gradients (Sigma) were used to purify the islets that were then handpicked under a dissecting microscope. Triplicates of ten islets each were incubated in Kreb's Ringer Buffer containing the indicated concentrations of glucose. After 60 minutes at 37ºC, the supernatant was collected and insulin levels measured using an Insulin ELISA Kit (Chrystal Chem). After collecting the supernatant, islets were collected and DNA concentration was measured and used to normalize the measured insulin secretion given the

intrinsic variation in islet size. Measurement of *in vivo* fatty acid oxidation was performed with ^{14}C-labeled oleic acid as previously described (Gautam et al., 2006). Indirect calorimetry was performed at room temperature using an eight-chamber Oxymax system (Columbus Instruments) (Chen et al., 2009). Mice were acclimated for one day in the metabolic chamber before any assessments were made. Motor activities were determined by infrared beam interruption (Opto-Varimex mini; Columbus).

Barnes Maze Testing:

To assess spatial learning and memory we employed the Barnes maze test (Kennard and Woodruff-Pak, 2011). This apparatus consists of a 91 cm diameter grey circular plate elevated 90 cm above the floor containing twenty identical holes, five cm in diameter, evenly spaced across the maze's circumference (Stoelting Co., Illinois). An escape box, a small dark recessed chamber, was located under one of the 20 identical holes and was assigned as the goal box. Visual cues of different shapes and colors were attached to the walls surrounding the maze. The principle of the test is that the mice will utilize the visual cues as they learn to locate and enter the goal box in order to escape the aversive environment of the maze surface where they are exposed to bright lights, a high frequency auditory tone stimuli, and air blowing from fans placed above the maze. Mice were tested over five consecutive days with 4 trials per day. Decreased latencies to enter the goal box over consecutive days of testing, decreased number of erroneous nose pokes into incorrect (non target box) holes and the transition time from random hole searches to predominately strategic approaches to locating the goal box were used as indices of spatial learning and memory. We used 6 young female WT mice (mean age 6.0 ± 0.2 months) and 6 young female mTOR$^{\Delta/\Delta}$ mice (mean age 5.0 ± 0.3) along with 9 old female WT mice (mean age 18.8 ± 1.1 months) and 13 old female mTOR$^{\Delta/\Delta}$ mice (mean age 19.1 ± 0.8 months).

Strength, Coordination, Gait analysis and Bone density:

Forearm grip strength was evaluated in mice with a Grip Strength Meter (Columbus Instruments, Columbus OH). Mice were brought to the test room and allowed to acclimate prior to testing. To measure forearm limb grip strength, the mice were held by the base of the tail and allowed to grasp a horizontally oriented metal pull grid with their front paws. The experimenter gently and steadily pulled the mice backwards with the torso aligned horizontally with the pull grid. The force (kilogram force) applied against the grid to the bar at the moment of grip release was recorded as peak tension. Five trials were performed for each mouse with a rest interval of 10 minutes between trials. Mean peak tension for the five trials was calculated. Grip strength was then normalized for body weight as grams of force/grams of body weight. We used 6 young female WT mice (mean age 6.3 ± 0.2 months) and 6 young female mTOR$^{\Delta/\Delta}$ mice (mean age 6.0 ± 0.3 months) along with 4 old female WT mice (mean age 24.7 ± 0.5 months) and 11 old female mTOR$^{\Delta/\Delta}$ mice (mean age 23.8 ± 0.3 months).

Motor coordination was evaluated with using a Rotamex-5 four lane Rotarod (Columbus Instruments, Columbus OH) consisting of a 3 cm diameter ridged plastic rotary rod positioned 60 cm above the table. On day 1, the mice were acclimated to the testing environment by placing them on the stationary rotary rod. The mice received two acclimation trails separated by a one hour rest interval. On day two, the mice were habituated to a slowly rotating rod (4 rpm) for three 300 sec trials with a one hour rest interval. The testing phase occurred 24 hours after habituation when the mice were placed on a rod programmed to accelerate from 4-40 rpm. The testing session consisted of three 300 sec trials separated by 1 hour rest intervals. Latency to fall off the rotating rod was detected by photo-detectors and automatically recorded along with the acceleration speed at the time of falling. We analyzed 6 WT young male mice (mean age 3.5 ± 0.2 months) and 6 young male $mTOR^{\Delta/\Delta}$ mice (mean age 3.6 ± 0.2) along with 4 old male WT mice (mean age 17.2 ± 0.8 months) and 7 old male $mTOR^{\Delta/\Delta}$ mice (mean age 17.6 ± 0.5 months).

For gait assessment, video recordings of the underside of mice ambulating at a constant speed (24 cm/s) were obtained using a transparent treadmill belt positioned above a high-speed digital camera (DigiGait Imaging System, Mouse Specifics, Boston MA). Videos capturing 3-4 continuous seconds in which the mice walked without stumbling and maintained a consistent position on the belt for a minimum of 10 consecutive strides were subsequently analyzed for multiple spatial and temporal gait parameters through the DigiGait Image Analysis System software. The DigiGait Imaging and Analysis system is based on ventral plane videography, and proprietary software that digitizes paw images and calculates the areas of approaching and retreating paws relative to belt and camera frame by frame as previously described (Piesla et al., 2009; Vincelette et al., 2007). We used 6 WT young female mice (mean age 6.1 ± 0.2 months) and 6 young female $mTOR^{\Delta/\Delta}$ mice (mean age 5.8 ± 0.3 months). For studies on older mice we used 6 WT mice (4 males and 2 females, mean age 20.3 ± 0.7 months) and 13 old $mTOR^{\Delta/\Delta}$ mice (6 males and 7 females, mean age 20.4 ± 0.4 months). We observed no difference in this parameter between males and female mice (for $mTOR^{\Delta/\Delta}$ old mice: stride width variance equals .30 ± .05 (n=6 male mice) and for female old mice 0.28 ± .03 (n=7 female mice), p=0.65)

For analysis of bone volume, bones from the hind legs of female mice were isolated and fixed in 4% paraformaldehyde-PBS overnight and stored prior to analysis in 70% ethanol. Micro CT (1172 high resolution micro-CT) was used along with the CTAnalyzer software package (Skyscan) to measure trabecular bone volume and total tissue volume of the isolated tibia (Ravoori et al., 2010). We used 4 young female WT mice (mean age 3.9 ± .3 months) and 4 young $mTOR^{\Delta/\Delta}$ mice (mean age 4.0 ± .5 months) along with 6 old female WT mice (mean age 24.9 ± 1.5 months) and 6 old female $mTOR^{\Delta/\Delta}$ mice (mean age 26.7 ± 0.9 months).

Supplemental References:

Chen, M., Wang, J., Dickerson, K.E., Kelleher, J., Xie, T., Gupta, D., Lai, E.W., Pacak, K., Gavrilova, O., and Weinstein, L.S. (2009). Central nervous system imprinting of the G protein G(s)alpha and its role in metabolic regulation. Cell Metab *9*, 548-555.

Gautam, D., Gavrilova, O., Jeon, J., Pack, S., Jou, W., Cui, Y., Li, J.H., and Wess, J. (2006). Beneficial metabolic effects of M3 muscarinic acetylcholine receptor deficiency. Cell Metab *4*, 363-375.

Kennard, J.A., and Woodruff-Pak, D.S. (2011). Age sensitivity of behavioral tests and brain substrates of normal aging in mice. Front Aging Neurosci *3*, 9.

Liu, J., Cao, L., Chen, J., Song, S., Lee, I.H., Quijano, C., Liu, H., Keyvanfar, K., Chen, H., Cao, L.Y.*, et al.* (2009). Bmi1 regulates mitochondrial function and the DNA damage response pathway. Nature *459*, 387-392.

Piesla, M.J., Leventhal, L., Strassle, B.W., Harrison, J.E., Cummons, T.A., Lu, P., and Whiteside, G.T. (2009). Abnormal gait, due to inflammation but not nerve injury, reflects enhanced nociception in preclinical pain models. Brain Res *1295*, 89-98.

Ravoori, M., Czaplinska, A.J., Sikes, C., Han, L., Johnson, E.M., Qiao, W., Ng, C., Cody, D.D., Murphy, W.A., Do, K.A.*, et al.* (2010). Quantification of mineralized bone response to prostate cancer by noninvasive in vivo microCT and non-destructive ex vivo microCT and DXA in a mouse model. PLoS One *5*, e9854.

Vincelette, J., Xu, Y., Zhang, L.N., Schaefer, C.J., Vergona, R., Sullivan, M.E., Hampton, T.G., and Wang, Y.X. (2007). Gait analysis in a murine model of collagen-induced arthritis. Arthritis Res Ther *9*, R123.

Wu, J.J., Roth, R.J., Anderson, E.J., Hong, E.G., Lee, M.K., Choi, C.S., Neufer, P.D., Shulman, G.I., Kim, J.K., and Bennett, A.M. (2006). Mice lacking MAP kinase phosphatase-1 have enhanced MAP kinase activity and resistance to diet-induced obesity. Cell Metab *4*, 61-73.

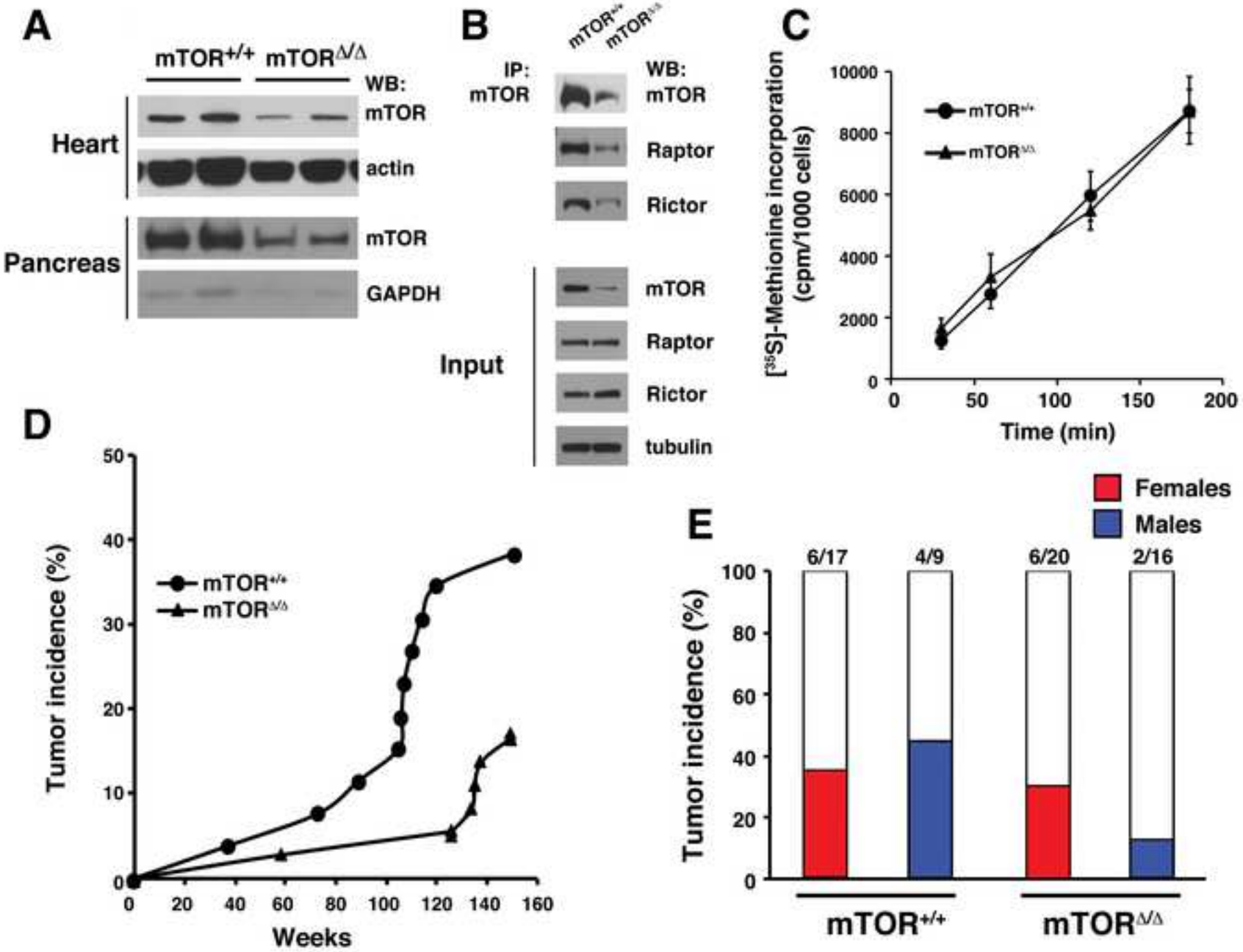
A
mTOR+/+
mTORΔ/Δ
WB:
Heart
mTOR
actin
Pancreas
mTOR
GAPDH
B
IP:
mTOR
WB:
mTOR
Raptor
Rictor
Input
mTOR
Raptor
Rictor
tubulin
C
[35S]-Methionine incorporation (cpm/1000 cells)
Time (min)
mTOR+/+
mTORΔ/Δ
D
Tumor incidence (%)
Weeks
mTOR+/+
mTORΔ/Δ
E
Females
Males
Tumor incidence (%)
6/17
4/9
6/20
2/16
mTOR+/+
mTORΔ/Δ

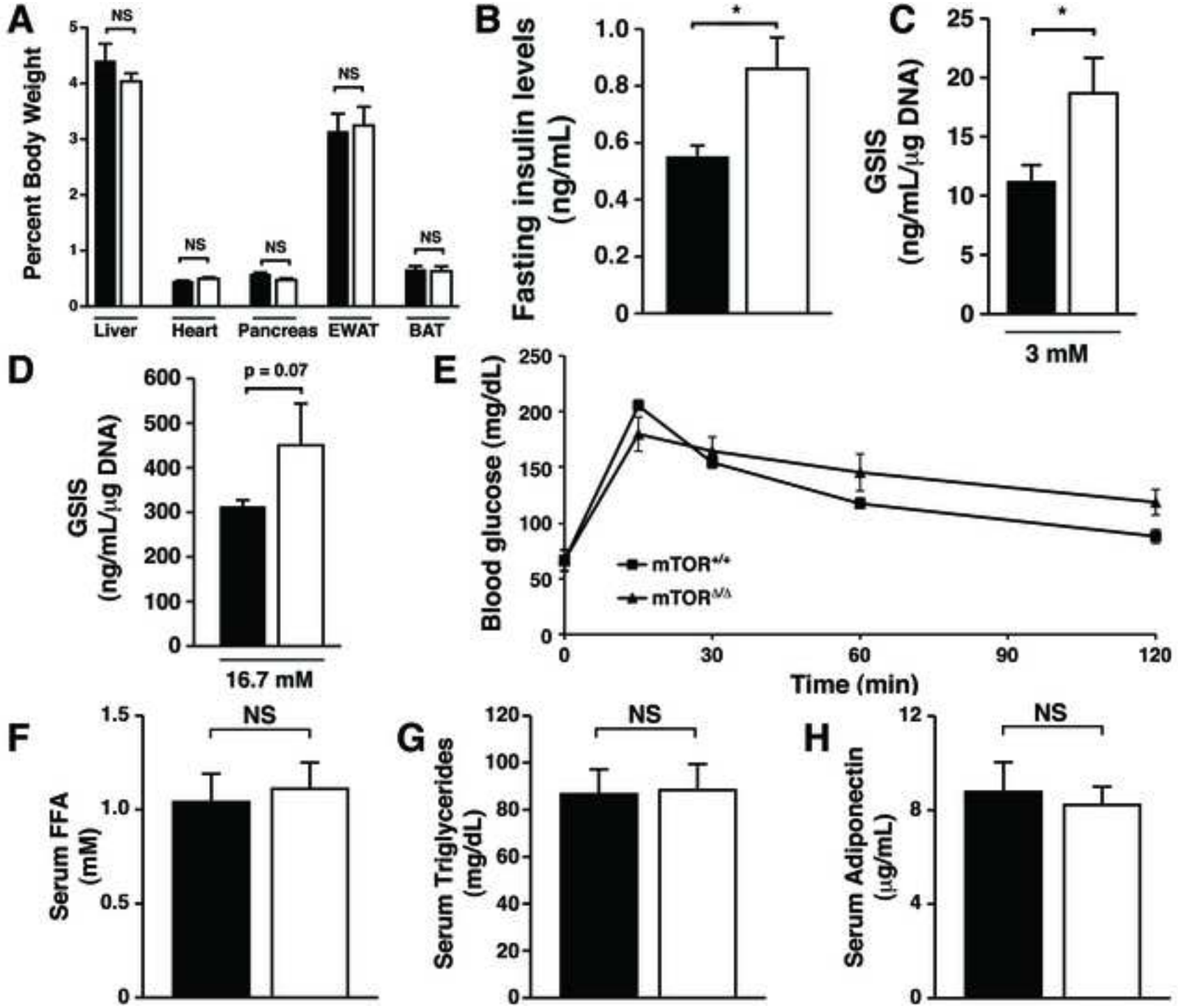
A
Percent Body Weight
NS
Liver
Heart
Pancreas
EWAT
BAT
B
Fasting insulin levels (ng/mL)
*
C
GSIS (ng/mL/μg DNA)
*
3 mM
D
GSIS (ng/mL/μg DNA)
p = 0.07
16.7 mM
E
Blood glucose (mg/dL)
mTOR+/+
mTORΔ/Δ
Time (min)
F
Serum FFA (mM)
NS
G
Serum Triglycerides (mg/dL)
NS
H
Serum Adiponectin (μg/mL)
NS

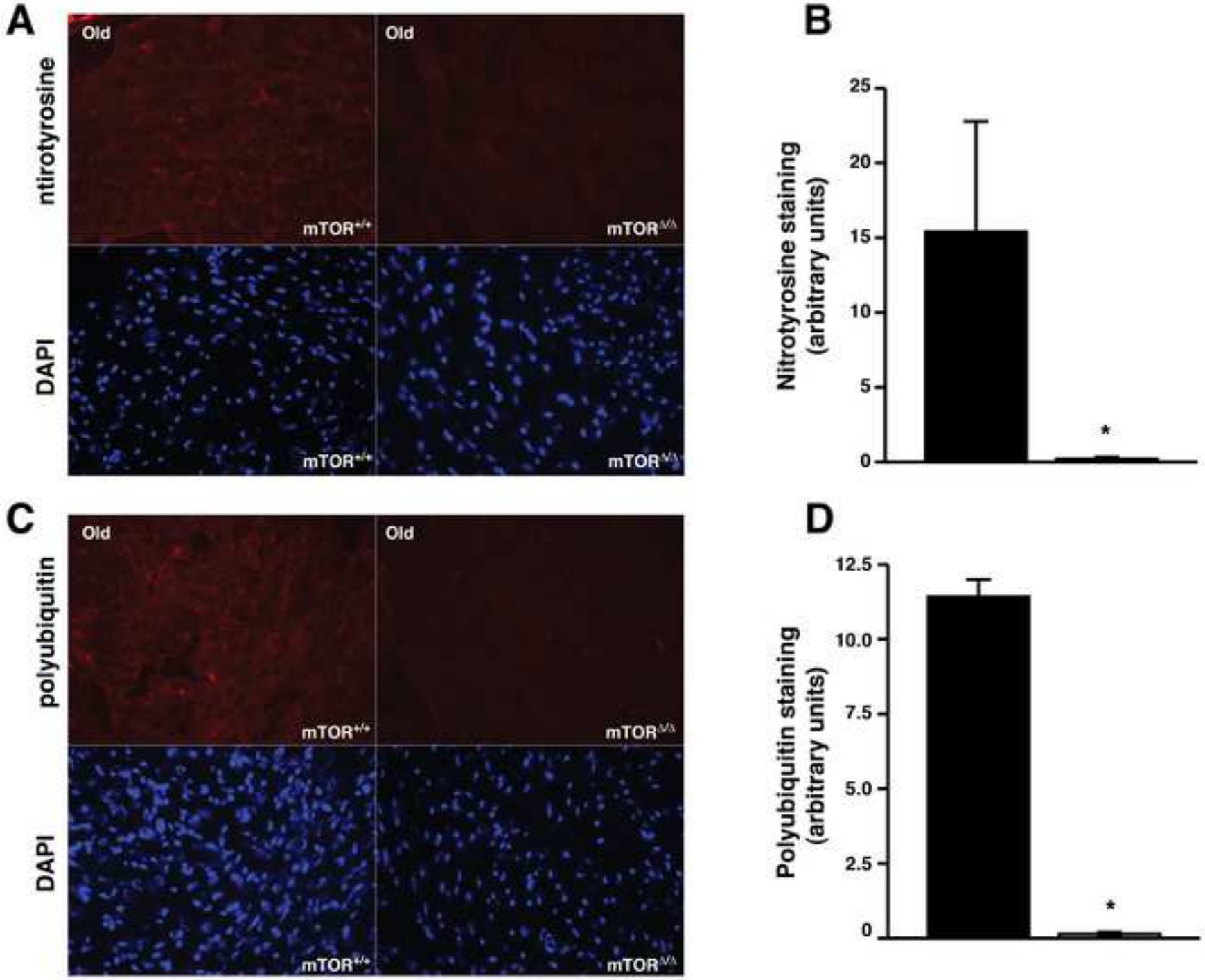
A
ntirotyrosine
DAPI
Old
Old
mTOR+/+
mTOR-/-
mTOR+/+
mTOR-/-
B
Nitrotyrosine staining
(arbitrary units)
25
20
15
10
5
0
*
C
polyubiquitin
DAPI
Old
Old
mTOR+/+
mTOR-/-
mTOR+/+
mTOR-/-
D
Polyubiquitin staining
(arbitrary units)
12.5
10.0
7.5
5.0
2.5
0
*

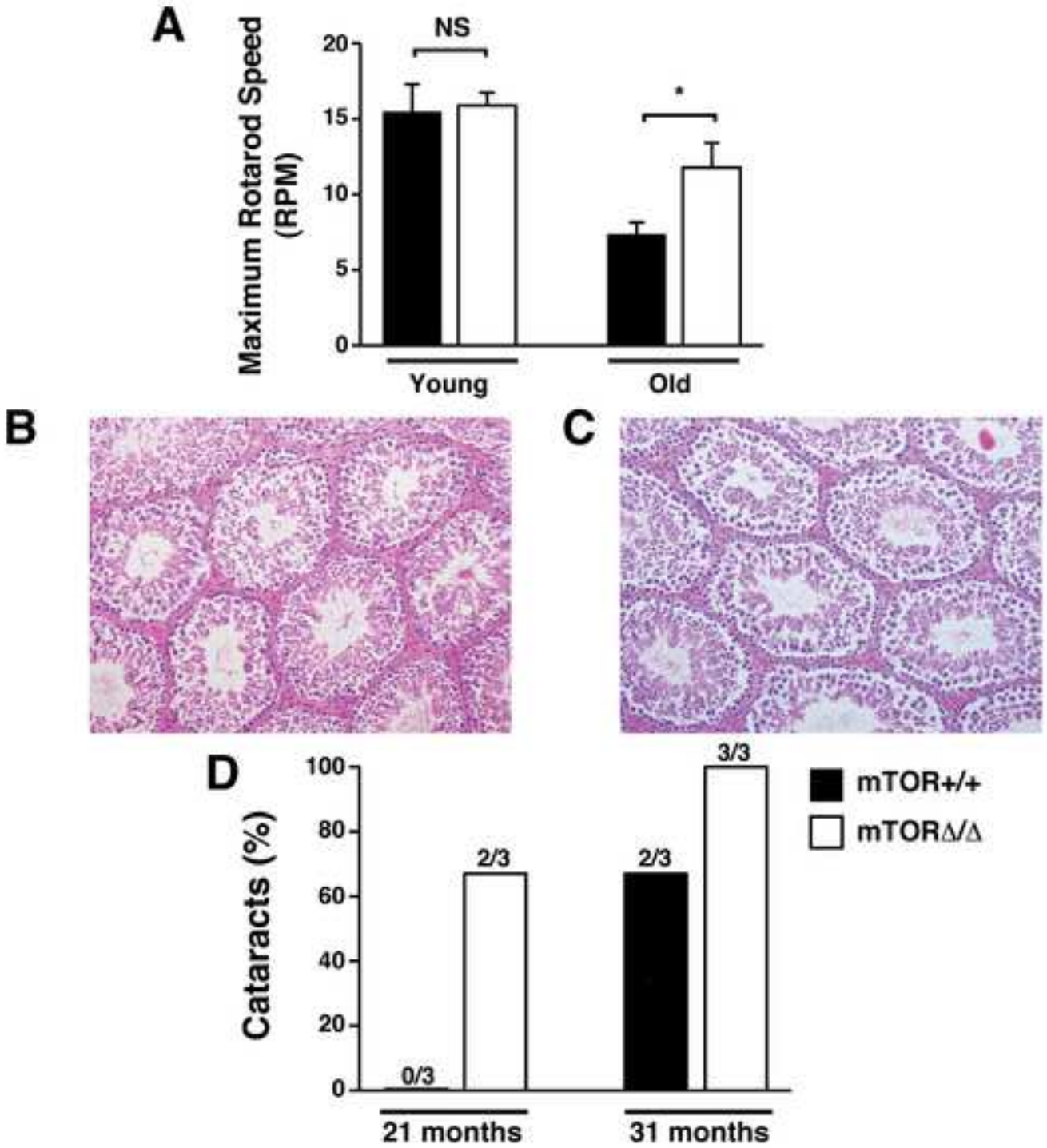
A
Maximum Rotarod Speed (RPM)
NS
*
20
15
10
5
0
Young
Old
B
C
D
Cataracts (%)
100
80
60
40
20
0
0/3
2/3
2/3
3/3
21 months
31 months
mTOR+/+
mTORΔ/Δ